# Vegetation drought monitoring from MODIS imagery and soil moisture data in Oklahoma Mesonet sites

## Monitoreo de sequía en la vegetación usando imagines de MODIS y datos de humedad del suelo en sitios de Oklahoma Mesonet

Diana X. Vanegas[1,2], Xiangming Xiao[1,2], Jeffrey Basara[3,4]


### Abstract

Drought is a normal and recurrent climatic phenomenon, and is considered one of the most costly natural disasters in the United States. Grassland vegetation is sensitive to weather and climate, and persistent drought impacts goods and ecological services that grasslands provide (e.g., wildlife habitats, feedstock for the livestock industry, and recreational services). Droughts have extremely large spatial and temporal variations in areal coverage and intensity making drought monitoring a challenging task. Using soil and atmospheric data from the Oklahoma Mesonet and surface reflectance data from the Moderate Resolution Imaging Spectroradiometer (MODIS) onboard the Terra and Aqua satellites, this study examined the hypothesis that the satellite-derived Land Surface Water Index (LSWI) is sensitive to drought conditions and can potentially be used as an indicator or tool for drought monitoring. The sensitivity of LSWI to summer drought was first analyzed at 10 Mesonet sites that are homogeneous and representative of different types of grassland vegetation, soils and climate across Oklahoma. A summer drought event is defined, based on threshold values of LSWI and the Fractional Water Index (FWI) derived from soil moisture data at each site.

### Resumen

La sequía es un fenómeno climático normal y recurrente, y es considerado uno de los desastres naturales más costosos en Estados Unidos. La vegetación de pastizales es sensible al estado del tiempo y el clima, y la persistencia de la sequía afecta a los bienes y servicios ecológicos que proporcionan los pastizales (por ejemplo, son hábitats de vida silvestre, proveen materia prima para la industria ganadera, así como servicios de esparcimiento). La cobertura de área e intensidad de las sequías presentan grandes variaciones espaciales y temporales, haciendo que el monitorea de sequías sea una tarea difícil. Usando datos atmosféricos y de suelos de la Oklahoma Mesonet, y datos de reflectancia de la superficie terrestre del espectrorradiómetro de imágenes de resolución moderada (MODIS, por sus siglas en inglés) a bordo de los satélites Terra y Aqua, este estudio examinó la hipótesis de que el índice de agua de la superficie del terreno (LSWI, por sus siglas en inglés) es sensible a condiciones de sequía y potencialmente puede utilizarse como un indicador o herramienta para la monitoreo de sequías. La sensibilidad del LSWI a la sequía estival se analizó inicialmente en 10 sitios Mesonet que son homogéneos y representativos de los diferentes tipos de vegetación de pastizales, los suelos


Acknowledgements: This work was supported, in part, from the NOAA Climate Program Office's Sectoral Applications Research Program (SARP) grant NA130AR4310122 and the Agriculture and Food Research Initiative Competitive Grant no. 2012-02355 from the USDA National Institute of Food and Agriculture.

**Recibido / Received:** Septiembre 13 de 2014 **Aprobado / Aproved:** Octubre 15 de 2014

**Tipo de artículo / Type of paper:** Investigación Científica y Tecnológica.

**Afiliación Institucional de los autores / Institutional Affiliation of authors:** 1. Department of Microbiology and Plant Biology, College of Art and Sciences, the University of Oklahoma, Norman, OK 73019, USA. 2. Center for Spatial Analysis, College of Atmospheric and Geographic Sciences, the University of Oklahoma, Norman, OK 73019, USA. 3. School of Meteorology, University of Oklahoma, Norman, OK 73072, USA. 4. Oklahoma Climatological Survey, University of Oklahoma, Norman, OK 73072, USA.

**Autor para comunicaciones / Author communications:** Diana X. Vanegas, dianaximena@gmail.com

*Los autores declaran que no tienen conflicto de interés.*

Secondly, the LSWI-based drought algorithm was evaluated at 103 Oklahoma Mesonet sites. Finally, the LSWI-based drought algorithm was used to map spatial patterns and temporal dynamics of drought-affected land surface during 2001-2010 across Oklahoma. The results from this study demonstrated the potential of LSWI-based drought algorithm for tracking and mapping drought-affected grassland vegetation in Oklahoma with 3% commission error in the Oklahoma Mesonet sites during 2001-2010.

**Keywords**: MODIS, vegetation drought monitoring, grassland, land surface water index.

y el clima a través de Oklahoma. Un evento de sequía estival se define, en base a los valores de umbral de LSWI y el Índice de Agua fraccional (FWI) derivado de los datos de humedad del suelo en cada sitio. Posteriormente, el algoritmo de sequía basado en LSWI se evaluó en 103 sitios Oklahoma Mesonet. Por último, se utilizó el algoritmo de sequía basado en LSWI para mapear los patrones espaciales y la dinámica temporal de la superficie de la tierra afectada por la sequía durante 2001-2010 a través de Oklahoma. Los resultados de este estudio demostraron el potencial del algoritmo de sequía basado en LSWI para el seguimiento y la cartografía de vegetación de pradera afectada por la sequía en Oklahoma con un 3% de error de comisión en los sitios Oklahoma Mesonet durante 2001-2010.

**Palabras Clave**: MODIS, Monitoreo de sequía en la vegetación, praderas, índice de Agua de la superficie del terreno

## Introduction

Grassland ecosystems cover approximately 40% of the Earth's terrestrial land surface [1], [2]. There are several areal estimates of grasslands in the United States, and approximately 50% of the total land surface in the United States (U.S.) is classified as grasslands [3], [4]. The Great Plains (GP) in the North America is one of the largest grassland regions in the world [5]. Grassland ecosystems provide valuable goods and ecological services. Under moderate grazing conditions, grasslands play an important role in the nutrient cycle and hydrologic cycle, and can store significant amounts of carbon [4], [2]. Grassland ecosystems provide forage and support the livestock industry. Grasslands are rich in plant biodiversity and are important habitats for wild birds, wildlife and pollinators. Furthermore, grasslands can provide several recreational services (e.g. aesthetic beauty, wildlife observation, and hunting areas) to the human society.

Drought, which is normal and recurrent climatic phenomenon in the Great Plains region, can affect landscapes and people at local to regional scales from short periods of time [6], [7], [8], to decadal scales such as the Dust Bowl of the 1930s [9], [10], [11]. Droughts often result in a decrease in dry matter production and seed yield [12], [13], which has socio-economic effects, and especially agricultural productivity. A reduction in crop yield is not only an economic loss to individual farmers, but also leads to a reduction of food supply to humans and a loss of feedstock to the livestock industry. The data collected at the National Drought Mitigation Center (NDMC) at the University of Nebraska have shown that the economic damage of drought is at least as expensive as hurricanes and floods, and drought is one of the most costly natural disasters in the United States [14].

Because drought events and intensity have large spatial and temporal variations, drought monitoring is a challenging task. Scientists and decision makers use drought information and derived indices or indicators to monitor moisture supply conditions and apply this information to different economic activities (e.g. agriculture, water supply for human services, livestock management). Meteorology-based drought indices are the most common tools used to monitor drought, due to the long-term record of precipitation data available. Meteorological drought indices such as the Palmer Drought Severity Index (PDSI; [15]) or the Standardized Precipitation Index (SPI; [16], [17]) are derived from point-based meteorological measurements collected at individual weather stations. Thus, these drought indices only yield broad-scale drought patterns and are most applicable for regions with sufficient weather stations.

The optical sensors in space-borne remote sensing platforms, such as the Moderate Resolution Imaging Spectroradiometer (MODIS), provide surface reflectance data that are associated with the biophysical and biochemical properties of vegetation and soils across local, regional and global scales. Time-series analysis of vegetation indices has become a very common approach to analyze vegetation dynamics and drought monitoring [18]. The initial approaches for drought detection by satellite data were based on the reduction of photosynthetic capacity, which is most commonly measured through the Normalized Difference Vegetation Index (NDVI) and is also associated with precipitation deficiency [19]. The surface reflectance, or the combined responses of reflective and thermal data, has also been used to detect and monitor droughts [20]. In addition to NDVI, NDVI anomaly, and standardized NDVI values, among other red-NIR bands algorithms, have been used to identify and monitor drought at different spatial scales [21], [22], [23], [24], [25], [26], [19], [27]. The land surface temperature (LST) derived from thermal infrared (TIR) band has also been used to monitor drought in combination with NDVI, based on the hypothesis that high LST values indicate soil moisture deficiencies and therefore stress in the vegetation canopy [28].

The Normalized Difference Water Index (NDWI; [29], a normalized ratio calculated from two near-infrared (NIR) channels centered approximately on 0.86 $\mu$m and 1.24 $\mu$m, has been used to monitor drought as it is sensitive to changes in liquid water content of vegetation canopies [18], [30], [14], [31]. Short-wave infrared spectral band (SWIR) is also sensitive to water content in canopy and soil surface. Several studies have calculated a water-related vegetation index that uses both NIR (841-876 nm) and SWIR band (2105 – 2155 nm) in MODIS sensors, namely NDWI [18], [14], [30]. Other studies used another SWIR band (1580 – 1750 nm) and NIR band (841-876 nm) to calculate the Land Surface Water Index (LSWI) [32], [33]. LSWI, calculated as a normalized ratio between near infrared (NIR: 0.87 – 0.89 $\mu$m) and short-wave infrared (SWIR: 1.58 – 1.75 $\mu$m) spectral band, has been used to assess the impact of water stress on gross primary production of forests and croplands [34], [33].

In this study we examined the hypothesis that LSWI is sensitive to drought conditions and can be used as a drought monitoring indicator. We used in-situ soil moisture data from the Oklahoma Mesonet (Figure 1). Commissioned in 1994, the Oklahoma Mesonet is a network of over 110 automated weather stations with an average station spacing of approximately 30 km. Measurements collected at these stations include precipitation, air temperature, relative humidity, wind speed, solar radiation as well as soil moisture. The Oklahoma Mesonet calculates the fraction water index (FWI) in the soils, which is a relative measure of the soil wetness [14], [35], [36] and provides daily FWI data available to the public. We compared LSWI and FWI data at grassland sites during the warm season over the period of 2001-2010. The specific objectives of this study are (1) evaluate the relationship between LSWI and soil moisture (FWI); (2) use the LSWI as vegetation health indicator; and (3) use LSWI as a drought monitoring tool to map drought across the state of Oklahoma.

***Figure 1.*** *Spatial distribution of Oklahoma Mesonet sites*

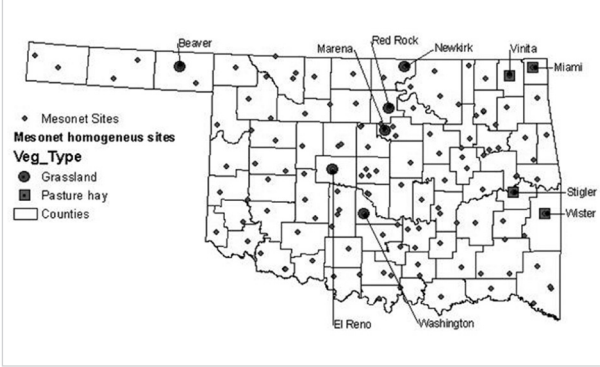


# Materials and methods

## The Oklahoma Mesonet data

The Oklahoma Mesonet is a network of environmental monitoring stations designed and implemented by scientists at the University of Oklahoma and Oklahoma State University [37]. The Mesonet network consists of over 110 automated stations (at least 1 Mesonet station in each of 77 counties) in Oklahoma (Figure 1). The Oklahoma Mesonet network has soil moisture sensors installed at various soil depths depending on ambient soil conditions at a station, for example, 5-cm sensors (103 stations), 25-cm sensors (101 sites), 60-cm sensors (76 sites), and 75-cm sensors (53 sites) [36].

***Table 1.*** *General characteristics of the 10 Oklahoma Mesonet sites*

| Site Name | Site ID | Latitude | Longitude | Vegetation | Soil type | Annual Precipitation (mm) 2001-2010 | |
|---|---|---|---|---|---|---|---|
| | | | | | | Mean | STD |
| Beaver | BEAV | 36.8025 | -100.530 | Grassland | Loam | 487 | 95 |
| El Reno | ELRE | 35.5485 | -98.0365 | Grassland | Silt loam | 788 | 244 |
| Marena | MARE | 36.0643 | -97.2127 | Grassland | Sandy clay loam | 881 | 227 |
| Miami | MIAM | 36.8883 | -94.8444 | Pasture/hay | Silt loam | 1046 | 240 |
| Newkirk | NEWK | 36.8981 | -96.9103 | Grassland | Silt clay loam | 905 | 228 |
| Red Rock | REDR | 36.3559 | -97.1531 | Grassland | Clay loam | 935 | 295 |
| Stigler | STIG | 35.2653 | -95.1812 | Pasture/hay | Silt loam | 1028 | 202 |
| Vinita | VINI | 36.7754 | -95.2209 | Pasture/hay | Silt loam | 1038 | 262 |
| Washington | WASH | 34.9822 | -97.5211 | Grassland | Sandy clay loam | 860 | 223 |
| Wister | WIST | 34.9843 | -94.6878 | Pasture/hay | Silt loam | 1127 | 249 |

We selected 10 MESONET sites for detailed analysis, including 6 grassland sites (Beaver, El Reno, Marena, Newkirk, Red Rock, and Washington) and 4 pasture/hay sites (Miami, Stigler, Vinita, and Wister). Table 1 summarizes the general characteristics of these sites, compiled from aerial images, a topographic map and detailed soil characteristics listed in the metadata for each Mesonet site.

These 10 sites are representative locations of the different soil types and climate zones across Oklahoma, and are homogeneous based on visual assessment of land cover from high-resolution imagery in Google Earth and analysis of the spatial variability of vegetation types within a 500 m buffer of each study site [14].

## MODIS surface reflectance data and vegetation indices

The Moderate Resolution Imaging Spectrometer (MODIS) is an instrument deployed on the NASA's Terra (EOS am) and Aqua (EOS pm) spacecraft that provides simultaneous observations of the atmosphere, land, and oceans at a temporal resolution of one to two days with high radiometric resolution images (12 bit). It collects data for 36 spectral bands; 7 bands are designated mainly for land surface and vegetation studies: blue (459-479 nm), green (545-565 nm), red (620-670 nm), near infrared (nir1: 841-875 nm and nir2: 1230-1250 nm), and shortwave infrared (swir1: 1628-1652 nm, and swir2: 2105-2155 nm) [38].

The 8-day MODIS land surface reflectance product (MOD09A1) at 500-m spatial resolution was used in this study. The MOD09A1 products are generated in a multi-step process that first eliminates observations with a low observational coverage, and then selects an observation with the minimum blue band value during an 8-day period. Reflectance values in the blue band are used to identify cloud cover and aerosols in the atmosphere that affect surface reflectance value and vegetation indices. Thus, the reflectance values reported in this product correspond to the observation with better overall pixel quality and observational coverage during each 8-day period [39].

The MOD09A1 time series datasets for individual Mesonet sites were downloaded from the data portal managed by the Earth Observation and Modeling Facility at the University of Oklahoma, which provides an on-demand visualization system for retrieving time series of MODIS data for a single site (http://eomf.ou.edu/visualization). The geographic locations of the Mesonet sites were used to retrieve MODIS data at pixel level. We used quality

*Table 2. Vegetation indices used in this study*

| Vegetation Index | Equation | MODIS Bandwidth (nm) | Reference |
|---|---|---|---|
| Normalized Difference Vegetation Index | $NDVI = \frac{\rho_{nir1} - \rho_{red}}{\rho_{nir1} + \rho_{red}}$ | red (620-670), nir1(841-875) | (Asrar et al. 1984) |
| Enhanced Vegetation Index | $EVI = 2.5x \frac{\rho_{nir1} - \rho_{red}}{\rho_{nir1} + 6x\,\rho_{red} - 7.5x\,\rho_{blue} + 1}$ | blue (459-479), red (620-670) , nir1(841-875) | (Xiao et al. 2004a) |
| Land Surface Water Index | $LSWI = \frac{\rho_{nir1} - \rho_{swir1}}{\rho_{nir1} + \rho_{swir1}}$ | nir1(841-875) swir1 (1628-1652) | (Xiao et al. 2004a) |
| Normalized Difference Water Index | $NDWI = \frac{\rho_{nir1} - \rho_{nir2}}{\rho_{nir1} + \rho_{nir2}}$ | nir1(841-875), nir2(1230-1250) | (Gao 1996) |
| Normalized Burn Ratio | $NDWI = \frac{\rho_{nir1} - \rho_{swir2}}{\rho_{nir1} + \rho_{swir2}}$ | nir1(841-875), swir2 (2105-2155) | (Lozano et al. 2010) |

flags (cloud, cloud shadow, aerosols) of observations in the dataset to exclude bad-quality observation. We also applied an additional filter to remove cloudy observations using a threshold value (≥0.20) of blue band reflectance during the plant growing season. The observations above this threshold were gap-filled following the same method reported in previous studies of MODIS-based land surface phenology [40], [41], [33], [42]. After this pre-procesing step, for each MODIS 8-day composite, surface reflectance values for blue, red, near infrared and shortwave infrared bands were used to calculate NDVI, EVI, LSWI, NDWI, and NBR (see Table 2).

## Drought detection and mapping – FWI-based and LSWI-based algorithms

Soil moisture data are used to calculate the fractional water index (FWI) [43], which is a unitless and linear index based on the response from the Campbell Scientific 229-L sensor installed at the Mesonet sites. FWI value varies from zero (very dry soil) to one (saturated soil). The results from a previous study [35] showed that FWI has distinct seasonal dynamics across Oklahoma, characterized by four "phases" or "periods" throughout the year (Figure 2). The 1st FWI phase is "moist plateau" in winter (November – mid March). It has the highest FWI values and vegetation is dormant due to low temperature values. The 2nd FWI phase is "transitional drying" during the climatological wet season in Oklahoma (mid-March to mid-June). The 3rd FWI phase is "enhanced drying" in mid-June to late August. It includes a steep decline of FWI values at all soil-depth levels, and the lowest FWI values occur during late summer because limited moisture replenishment to the soil due to minimal precipitation and enhanced evapotranspiration. The 4th FWI phase is "recharge phase" (late August to November), and large amount of precipitation and low evapotranspiration in autumn replenishes soil moisture. Reference [35] suggested that grassland vegetation in Oklahoma begins to wilt due to soil moisture deficits when FWI values are approximately 0.5, and if FWI values reached 0.3 or less, vegetation started to die. In this study we use FWI $<=$ 0.5 as the threshold value for FWI-based drought and values at 25-cm and 60-cm soil depths in July – August for individual sites were analyzed, respectively. If FWI values during an 8-day period reached $<=$ 0.5, this 8-day period is then considered to be "drought" period; otherwise, it is labeled as "non-drought" period. For each year, if there is one or more "drought" period within July-August, this summer (year) is labeled as "drought year"; otherwise, it is labeled as "non-drought year".

***Figure 2.*** *Seasonal dynamics of fractional water index (FWI), which were averaged over 58 Mesonet stations in Oklahoma. It illustrates four soil moisture phases (I–IV). It is from Illston et al. 2004.*

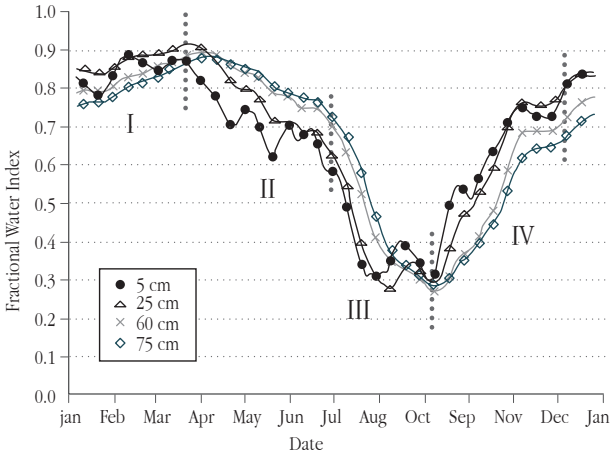


Green vegetation has positive LSWI values, but senescent vegetation and soils have negative LSWI values. Severe drought conditions often result in senescence of vegetation. In this study, we use the threshold of LSWI $<0$ as the indicator for vegetation drought during the plant growing season. LSWI values in July – August for individual sites were analyzed. If LSWI value in an 8-day period reached $<0$, this 8-day period is considered to be "drought" period; otherwise it is labeled as "non-drought" period. For each year, if there are one or more "drought" periods within July-August, this summer (year) is labeled as "drought year"; otherwise, it is labeled as "non-drought year".

We first applied the LSWI-based and FWI-based algorithms to the 10 grassland sites (Table 1), and then applied the algorithms to all the 103 Mesonet stations with soil moisture data over the period of July - August. We compared the results of drought and non-drought events from FWI-based (25 and 60 cm soil depths) and LSWI-based algorithms at individual sites, respectively. LSWI-based drought may agree with FWI (25 cm) drought only, FWI (60 cm) drought only, or both FWI (25 cm) and FWI (60 cm) drought, or neither. We applied the LSWI-based drought algorithm to all LSWI images in July – August during 2001-2010 and generated maps of "drought" and "non-drought" across Oklahoma. We then counted the total area affected by drought at each 8-day period, and evaluated changes in drought-affected areas in July-August over the study period.

# Results

## Seasonal dynamics of precipitation, soil moisture and vegetation indices at the Mesonet sites

We presented the data from El Reno and Marena sites (Table 1) to illustrate seasonal dynamics of precipitation, soil moisture and vegetation indices. Figure 3 shows the landscapes and the approximate MODIS pixel boundary at these two grassland sites. The El Reno site is largely pure grassland, and the Marena site has a small proportion of wood vegetation.

***Figure 3.*** *Landscape characteristics in (a). El Reno and (b). Marena Mesonet sites. The red box shows the MODIS pixel boundary (500-m spatial resolution) overlaid with Google Earth. From: http://daac.ornl.gov/cgi-bin/MODIS/GLBVIZ_1_Glb/modis_subset_order_global_col5.pl*

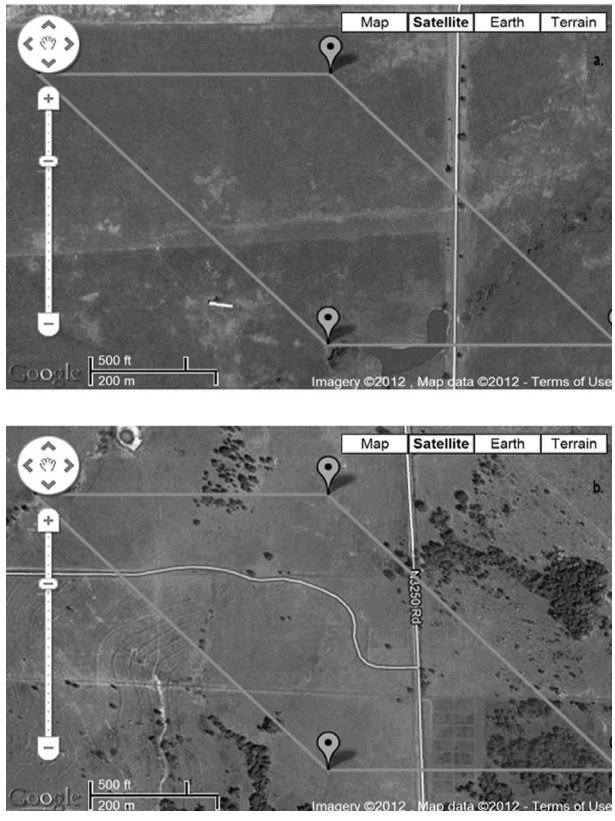


At the El Reno site, annual precipitation varied substantially, ranging from 473 mm in (2003) to 1370 mm in 2007 (Figure 4a). There were also large variations in seasonal

dynamics of precipitation. For example, 2001, 2004, 2008 and 2010 had small amounts of rainfall in previous winter and spring while 2003 and 2007 had the lowest amounts of rainfall in the period of July-August. The seasonal dynamics of soil moisture (FWI) at the 25 cm and 60 cm depths responded to seasonal dynamics of precipitation (Figure 4b). FWI-25cm values were high in spring but dropped below 0.5 in July-August period for 9 of the study years (the exception was 2007). The year 2006 had low FWI values over several months, and the "enhanced drying phase" lasted until November at the 25 cm depth and until January 2007 at the 60 cm soil layer. Both 2007 and 2008 were particularly wet years with values above 0.5 all year long in 2007 at both depths. During 2008, FWI values fell below 0.5 for just a few days in early August at the 25 cm soil depth and from late July to mid August at 60 cm soil depth. The seasonal dynamics of vegetation indices within the plant growing season (Figure 4c and d) corresponded well with that of precipitation and soil moisture. The greenness-related vegetation indices (NDVI and EVI) had the 1st (larger) peak in spring to early summer, a trough in July-August, and the 2nd (much smaller) peak in fall (Figure 4c). The water-related vegetation indices (LSWI, NDWI, and NBR) show similar seasonal pattern within the plant growing season, LSWI often reached its peak values in May or June and had its trough (-0.2) in July and September. The NDWI had peak values (~0.1) around late April or May, and the lower values (approximately -0.2) during august and in the winter. The NBR values in the warm season (May to September) remained positive during most of the years for the entire study period. The peak NBR values (>0.5) occurred in May and July and the trough NBR values (-0.1) occurred during the winter and few August periods on 2001-2003.

At the Marena site, annual precipitation varied substantially, ranging from 598 mm in 2006 to 1386 mm in 2007 (Figure 5a). The seasonal dynamics of precipitation was large and had large peaks in winter/spring and fall and a trough in July-August period. Soil moisture (FWI) at both 25-cm and 60-cm depths (Figure 5b) had distinct 4-phase dynamics of the FWI in most of years. FWI-25cm values were high in spring but dropped below 0.5 for all 10 years of the study. At the 25 cm depth, 2004 had a short dry spell during early June (a single 8-day period) and a drought from mid July to October (ten 8-day periods). The 2005 and 2007 periods were wet years with few dry spell or drought days between late July and August, and FWI values at 60 cm soil depth remained greater than 0.6 all for the duration of 2007. Year 2006 was a very dry year and both FWI-25cm and FWI-60cm values dropped below 0.5 for several months and did not recover until early 2007. The seasonal dynamics of greenness-related vegetation indices (NDVI and EVI) had a clear, single peak in early summer (Figure 5c). NDVI values had a plateau in most of summer, which reflects the fact that this site has fair amount of woody vegetation. The water-related vegetation indices also exhibited a single peak seasonal dynamics (Figure 5d)

***Figure 4.*** *Seasonal dynamics and interannual variation of precipitation, soil moisture and vegetation indices between 2001 and 2010 at Oklahoma Mesonet El Reno site. (a). Precipitation: each bin represents the accumulated rainfall measured in mm within each 8-day period. (b). Average daily fractional water index (FWI) at 25cm and 60 cm depth. (c). greenness-related vegetation indices: Normalized Difference Vegetation Index (NDVI), Enhanced Vegetation Index (EVI). (d). water-related vegetation indices: Land Surface Water Index (LSWI), Normalized Difference Water Index (NDWI) and Normalized Burn Ratio (NBR).*

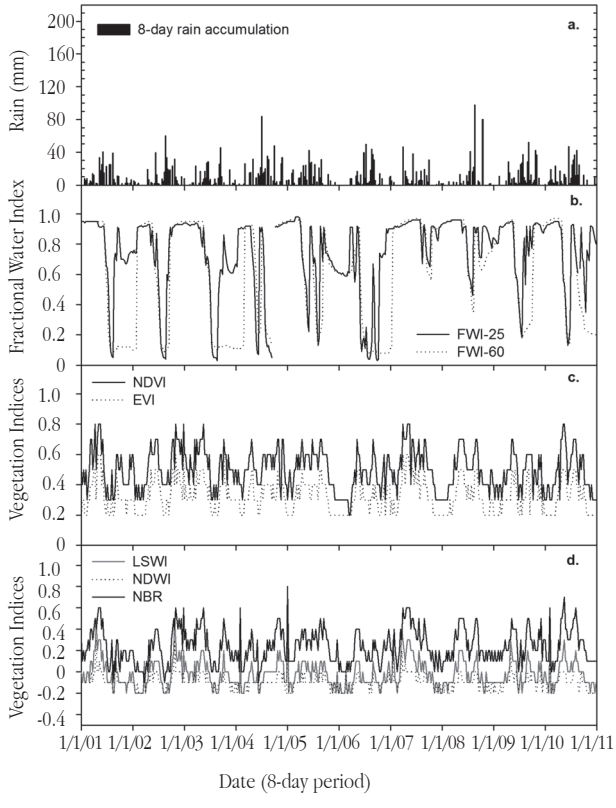

***Figure 5.*** *Seasonal dynamics and interannual variation of precipitation, soil moisture and vegetation indices between 2001 and 2010 at Oklahoma Mesonet Marena site. (a). Precipitation: each bin represents the accumulated rainfall measured in mm within each 8-day period. (b). Average daily fractional water index (FWI) at 25cm and 60 cm depth. (c). greenness-related vegetation indices: Normalized Difference Vegetation Index (NDVI), Enhanced Vegetation Index (EVI). (d). water-related vegetation indices: Land Surface Water Index (LSWI), Normalized Difference Water Index (NDWI) and Normalized Burn Ratio (NBR).*

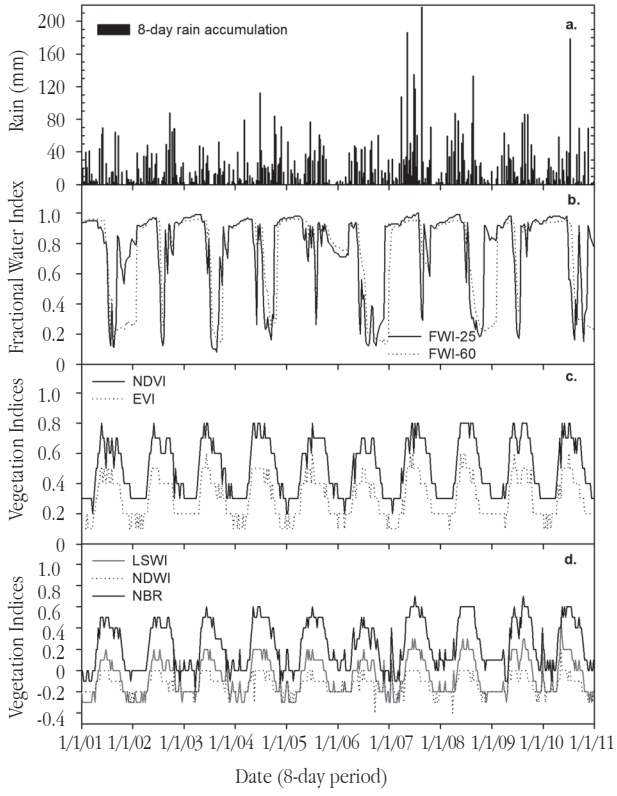


## Drought-affected areas identified by FWI- and LSWI-based algorithms at the Mesonet sites

We first applied the LSWI-based and FWI-based (both 25 and 60 cm soil depths) drought algorithms to the ten individual sites (see Table 1). Figure 6 illustrates the seasonal dynamics of LSWI and FWI at the El Reno site and the drought periods identified by the LSWI- and FWI-based drought algorithms. The LSWI-based drought algorithm identified drought periods in 10 years while the FWI-25cm algorithm identified drought in 8 years, and the FWI-60cm algorithm identified drought in 9 years. In comparison, at the Marena site, the LSWI-based drought algorithm identified drought periods in 3 years (2001, 2003 and 2006), but the FWI-25cm algorithm identified drought periods in 10 years, and the FWI-60 algorithm identified drought periods in 9 years. The discrepancy between LSWI-based drought detection and FWI-based drought detection could be attributed to the spatial domains size and landscape heterogeneity. Soil moisture measurements were taken as point measurements and represent a very small size of spatial domain (in meters), where vegetation is pure grassland. LSWI values from the MODIS sensor have a much larger spatial domain (500-m spatial resolution), where a mixture of grassland and trees exists. Trees did not defoliate in the summer in regular years, and only defoliated in those extreme drought years (e.g., 2001, 2003 and 2006), which resulted in very low LSWI values ($<0.0$).

***Figure 6.*** *Seasonal dynamics of fractional water index (FWI), land surface water index (LSWI), and drought events at the El Reno site during 2001-2010. Fractional Water Index data are from Oklahoma Mesonet soil moisture at 25 and 60 cm depth data. Land Surface Water Index (LSWI) data are calculated from 8-day MODIS land reflectance data. The green area demarks the plant growing season at the site. The gray bars highlight the drought periods (detected by both LSWI- and FWI-25 drought algorithms). The red lines mark the period when either temperature or water are the main controllers for vegetation health. FWI-25 – solid line; FWI-60 – dotted line; and LSWI – dash-dot line.*

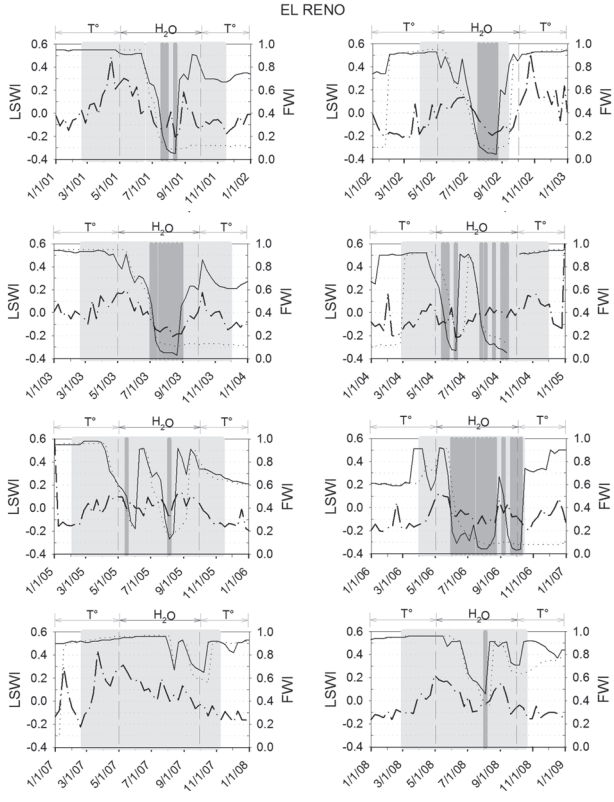

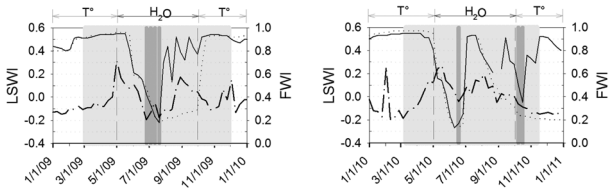


***Figure 7.*** *Seasonal dynamics of fractional water index (FWI), land surface water index (LSWI), and drought events at the Marena site during 2001-2010. Fractional Water Index data are from Oklahoma Mesonet soil moisture at 25 and 60 cm depth data. Land Surface Water Index (LSWI) data are calculated from 8-day MODIS land reflectance data. The green area demarks the plant growing season at the site. The gray bars highlight the drought periods (detected by both LSWI- and FWI-25 drought algorithms). The red lines mark the period when either temperature or water are the main controllers for vegetation health. FWI-25 – solid line; FWI-60 – dotted line; and LSWI – dash-dot line.*

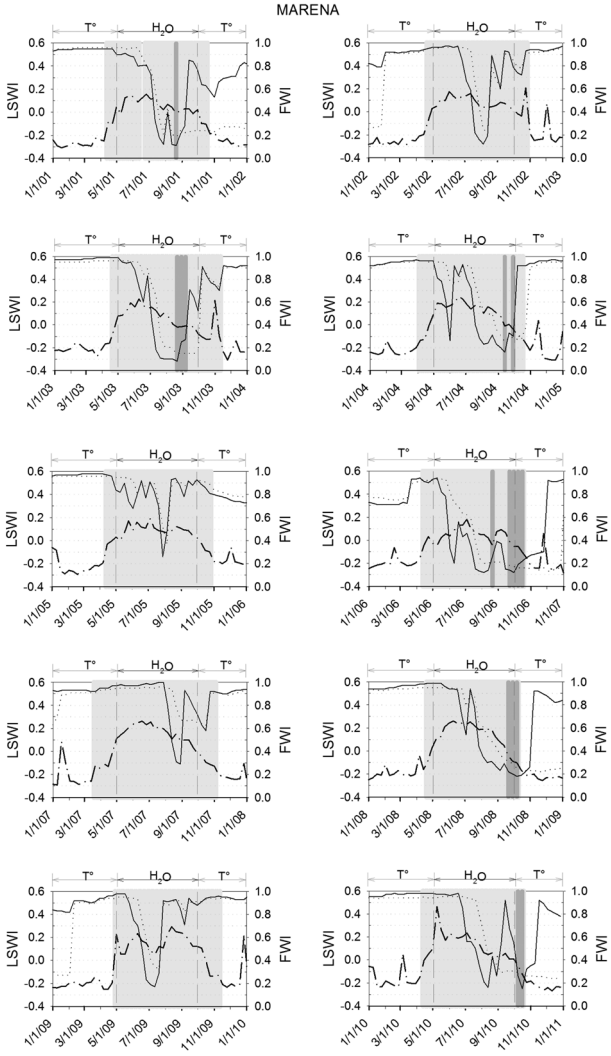


The results of drought detection from the FWI- and LSWI-based drought algorithms at the 10 sites during July and August of 2001-2010 are summarized in Table 3. On average for these 10 sites, 59% of the years had hits, but the standard deviation was high (31%). These 10 sites can be grouped in 2 groups: sites with more than 50% hits (Beaver, El Reno, Washington, Wister, Red Rock and Vinita); and sites with 40% hits or less (Newkirk, Stigler, Marena and Miami). The average hits for the first group was 80% with a standard deviation of 18%. The average hits for the second group was 28% with a standard deviation of 11%. This reflects to some degree the issues of spatial domain size and landscape heterogeneity between the FWI approach and LSWI approach.

***Table 3.*** *Drought detection at 10 Oklahoma Mesonet sites over the period of July-August during 2001-2010 by the LSWI- and FWI-based drought algorithms D-drought, ND – non-drought. This table is the result of a cross-site comparison by multilevel sorting of the 10 homogeneous sites so that those sites where LSWI and FWI yielded more hits will appear first. The first sorting level was by percentage of hits (descending), then by percentage of omission error or misses (ascending), and finally by commission error or false alarms (ascending).*

| Site | | | | FWI-25 cm | | FWI-60 cm | |
|---|---|---|---|---|---|---|---|
| | | | | D | ND | D | ND |
| Site ID | LSWI | D | # | Hit (D) | False alarm | Hit (D) | False alarm |
| | | ND | # | Miss | Hit (ND) | Miss | Hit (ND) |
| BEAV | LSWI | D | 9 | 9 | 0 | 6 | 3 |
| | | ND | 1 | 0 | 1 | 0 | 1 |
| ELRE | | ND | 0 | 0 | 0 | 0 | 0 |
| | | D | 8 | 8 | 0 | 6 | 2 |
| WASH | | D | 8 | 8 | 0 | 6 | 2 |
| | | ND | 2 | 1 | 1 | 1 | 1 |
| WIST | | D | 7 | 7 | 0 | 7 | 0 |
| | | ND | 3 | 3 | 0 | 3 | 0 |
| REDR | | D | 6 | 6 | 0 | 5 | 1 |
| | | ND | 4 | 4 | 0 | 3 | 1 |

| Site | | | | FWI-25 cm | | FWI-60 cm | |
|---|---|---|---|---|---|---|---|
| | | | | D | ND | D | ND |
| Site ID | LSWI | D | # | Hit (D) | False alarm | Hit (D) | False alarm |
| | | ND | # | Miss | Hit (ND) | Miss | Hit (ND) |
| VINI | LSWI | D | 5 | 5 | 0 | 5 | 0 |
| | | ND | 5 | 3 | 2 | 2 | 3 |
| STIG | | D | 3 | 3 | 0 | 3 | 0 |
| | | ND | 7 | 5 | 2 | 2 | 5 |
| NEWK | | D | 3 | 3 | 0 | 3 | 0 |
| | | ND | 7 | 6 | 1 | 7 | 0 |
| MARE | | D | 3 | 3 | 0 | 3 | 0 |
| | | ND | 7 | 7 | 0 | 6 | 1 |
| MIAM | | D | 1 | 1 | 0 | 1 | 0 |
| | | ND | 9 | 7 | 2 | 7 | 2 |

We also applied the FWI-25 and LSWI-based drought algorithms to all the Oklahoma Mesonet sites that have soil moisture measurements at 25-cm depth and 60-m depth, respectively. Figure 8a shows the total number of sites that had one or more drought periods within July-August in a year, based on the LSWI- and FWI-25cm drought algorithms. The agreement between the FWI-25cm algorithm and the LSWI algorithm is best in those dry years (2001, 2003 and 2006) but worst in those wet years (2007, 2008). The LSWI-based algorithm had only a few (3% averaged over 10 years) false alarms (commission error) about drought. Figure 8b shows the total number of sites that had one or more drought periods within July-August in a year, based on the LSWI- and FWI-60cm drought algorithms.

The agreement between the FWI-60cm algorithm and the LSWI algorithm is still best in those dry years (2001, 2003 and 2006), but worst in those wet years (2007, 2008). The LSWI-based algorithm had only a few (6% averaged over 10 years) false alarms (commission error) about drought.

*Figure 8. A comparison of drought detection by the LSWI- and FWI-based drought algorithms, when applied to all the Oklahoma Mesonet sites during 2001-2010. A site was considered as drought in a summer (year), if one or more 8-day periods between July and August were identified as drought period by the LSWI- or FWI-based drought algorithms: (a).* ***a comparison between LSWI and*** *FWI-25cm algorithms; and (b).* ***A comparison between LSWI and*** *FWI-60cm algorithm. The bars show (1) number of Mesonet sites identified as drought by FWI-based algorithm, (2) number of Mesonet sites identified as drought by LSWI-based algorithm, (3) hit or agreement in drought (# of sites identified as drought by both LSWI- and FWI-based drought algorithms); (4) miss or omission error (# of sites identified as non-drought period by the LSWI-based drought algorithm but as drought period by the FWI-based algorithm, (5) false alarms or commission error (# of sites identified as drought by the LSWI-based algorithm but as non-drought period by FWI-based drought algorithm), and (6) N/A (# of sites that have no FWI data available for comparison).*

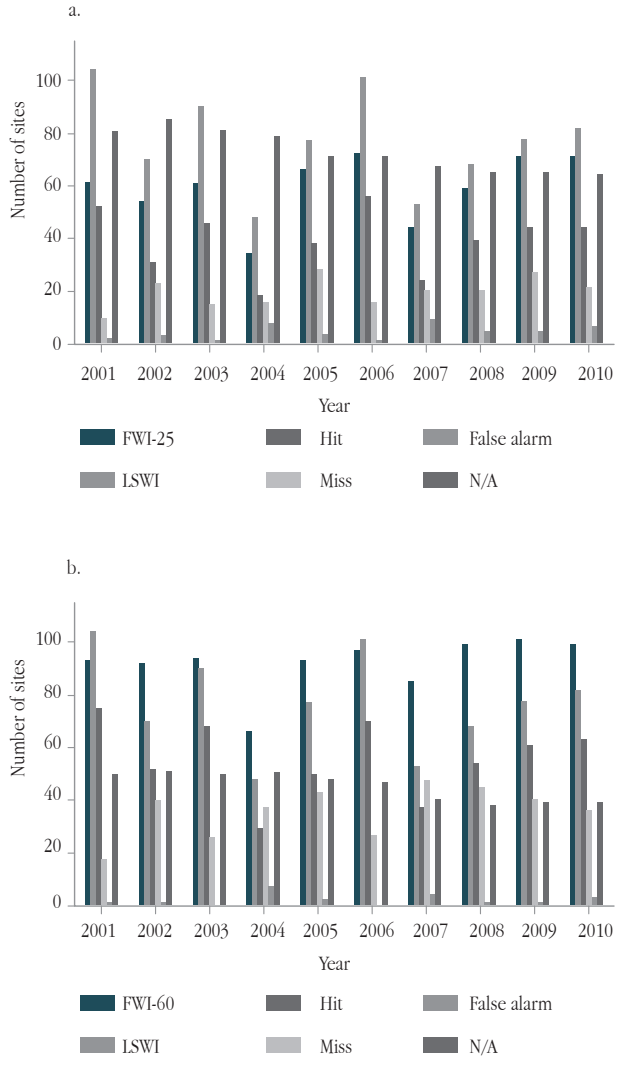

## Regional-scale mapping of drought-affected areas by LSWI-based drought algorithm

To quantify spatial patterns and temporal dynamics of drought-affected vegetation across Oklahoma, we applied the LSWI-based drought algorithm to all LSWI images. Figure 9 shows the spatial distributions of LSWI and FWI in July of 2006, 2007 and 2009 across Oklahoma. Year 2006 was a very dry year with an annual deficit in state-wide precipitation and drier than normal during all seasons [44]. Conversely, 2007 was a very wet year [44] while 2009 was a normal year in terms of annual precipitation for the state of Oklahoma. Monthly maps of FWI at 25-cm and 60-cm are derived from spatial interpolation of FWI at the Oklahoma Mesonet sites [37]. In comparison to the FWI maps, LSWI maps provide far more details on vegetation condition and drought-affected areas.

Figure 10 shows the changes in histogram of LSWI values in Oklahoma for all 8-day periods between July and August by year and table 4 summarizes the area under LSWI $<0$ by each 8-day period in these two months. Year 2009 is a normal year in terms of annual precipitation and seasonal distribution. The histogram distributions of LSWI values show that averaged over those 8-day periods in July-August, ~42% of MODIS pixels had negative LSWI values. On 4 July 2009, 45% of MODIS pixels in the state had negative LSWI values, and on July 20, 2009, 48% of MODIS pixels in the state had negative LSWI values, that are about 76,700 km2 of drought affected area. In the dry year 2006, more MODIS pixels had negative LSWI values and LSWI histogram distribution was skewed to the left side as a result of severe drought. The LSWI-based drought algorithm (LSWI $<$ 0) estimated ~100,700 km2 drought-affected area in mid-July (~63% of the total land area in the State) and ~113,500 km2 drought-affected area in mid-August (~70% of the total land area in the State). In the wet year 2007, more MODIS pixels had positive LSWI values and LSWI histogram distribution was skewed to the right side as the results of higher-than-normal rainfall. The LSWI-based drought algorithm (LSWI$<$0) estimated that only 21% of the State was considered to be drought-affected area by July 20, 2007. The drought-affected area increased slightly over time, and reached ~58,200 km2 (or ~36% of the state) by mid-August, 2007.

***Figure 9.*** *Spatial distributions of land surface water index (LSWI) and fractional water index (FWI) in Oklahoma in 2006, 2007 and 2009. Warm colors represent dry areas.* ***Top panel.*** *maps of land surface water index (LSWI) in 8-day period of July 20;* ***Middle panel.*** *maps of fractional water index (FWI) July daily average at 25-cm depth;* ***Lower panel:*** *maps of FWI July daily average at 60-cm depth.*

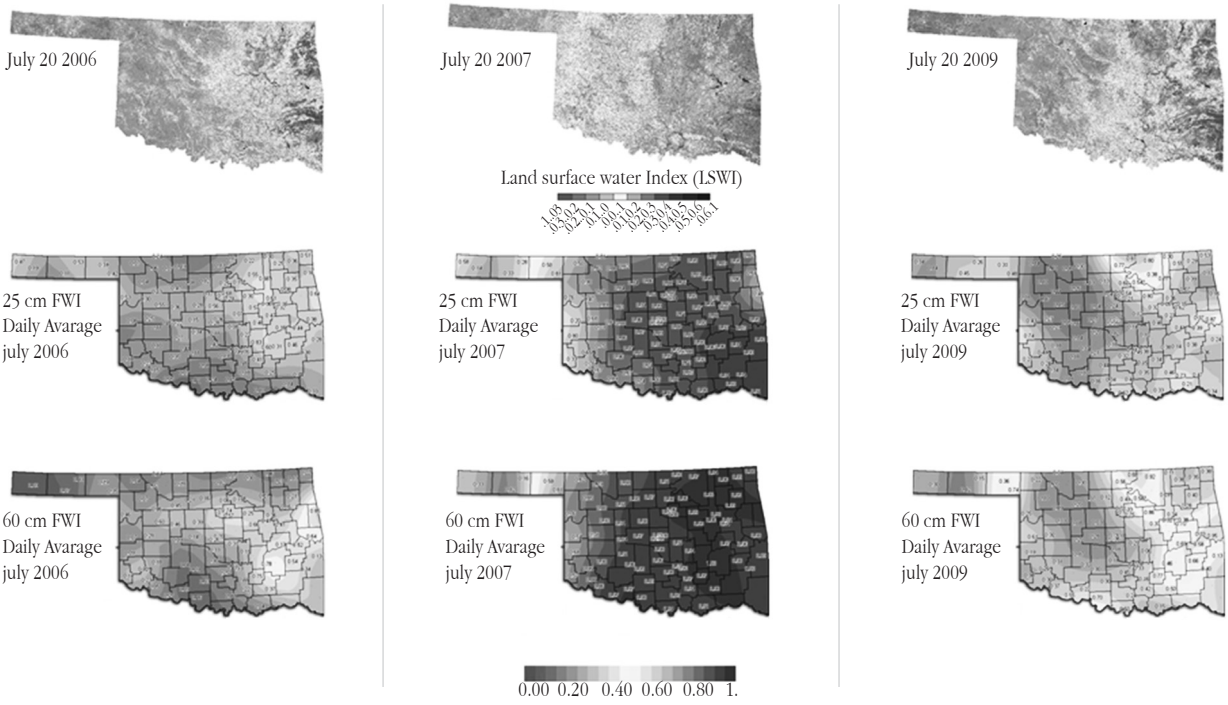

***Figure 10.*** *Changes in histograms of land surface water index (LSWI) in Oklahoma over the period of 4 July - 21 August during 2001-2010*

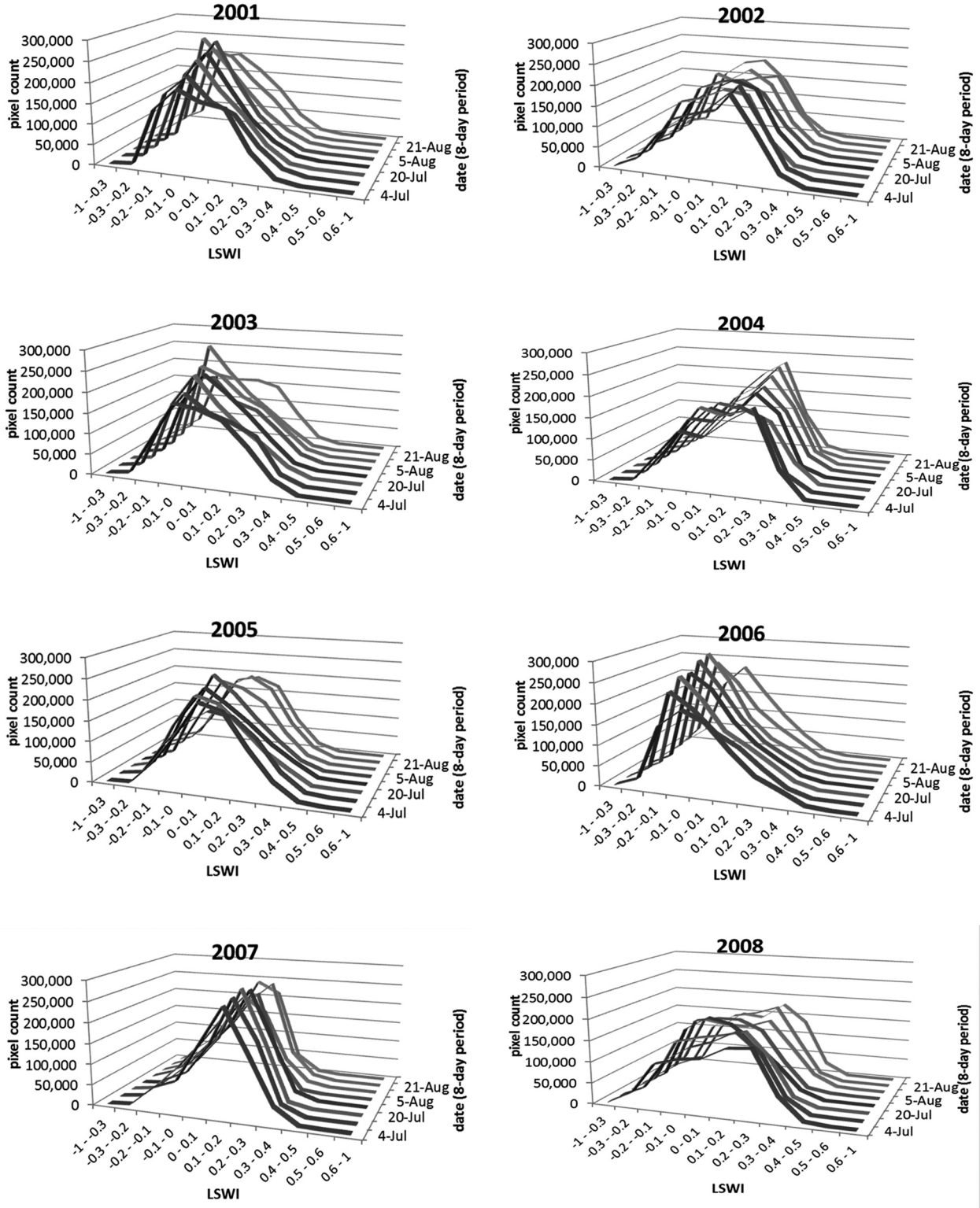

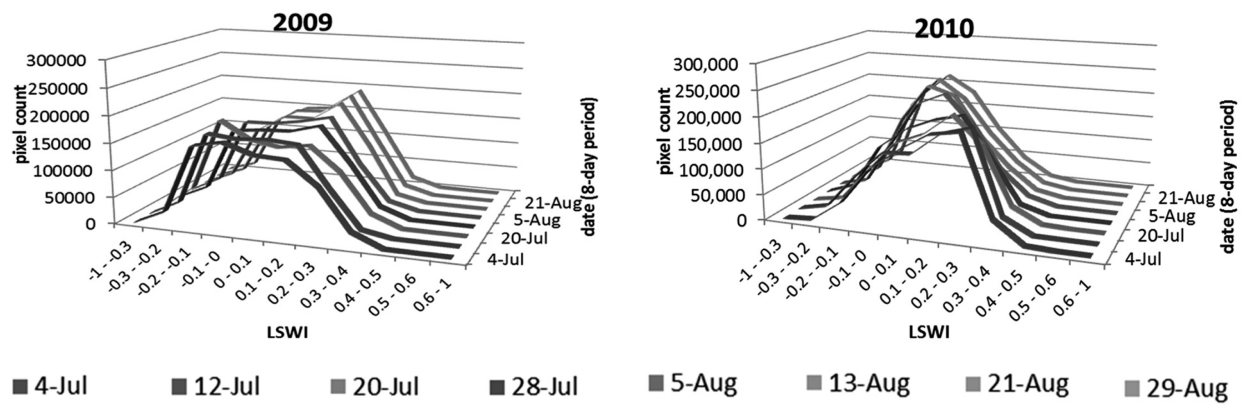


*Table 4. Vegetation drought affected areas (x103 km2) identified by the LSWI-based drought algorithm (LSWI < 0) during summer (July – August) of 2001-2010.*

| Year | July 4 | July 12 | July 20 | July 28 | Aug 5 | Aug 13 | Aug 21 | Aug 29 |
|---|---|---|---|---|---|---|---|---|
| 2001 | 74 | 83 | 88 | 97 | 100 | 107 | 100 | 90 |
| 2002 | 52 | 56 | 71 | 66 | 74 | 70 | 71 | 75 |
| 2003 | 62 | 71 | 83 | 80 | 86 | 90 | 102 | 77 |
| 2004 | 44 | 48 | 55 | 55 | 52 | 45 | 47 | 47 |
| 2005 | 40 | 50 | 70 | 75 | 78 | 70 | 57 | 63 |
| 2006 | 80 | 94 | 101 | 104 | 109 | 113 | 105 | 94 |
| 2007 | 28 | 29 | 34 | 35 | 47 | 58 | 48 | 53 |
| 2008 | 54 | 54 | 65 | 76 | 77 | 71 | 63 | 58 |
| 2009 | 73 | 74 | 77 | 68 | 70 | 63 | 61 | 61 |
| 2010 | 34 | 47 | 46 | 59 | 65 | 81 | 87 | 88 |

## Discussion

Vegetation indices derived from red and near infrared bands, for example, NDVI and Vegetation Condition Index (VCI), have been widely used and played an important role in vegetation drought monitoring [24], [45]. Recently, several studies [14], [30], [46] have used NDWI, which is a vegetation index derived from near infrared and shortwave infrared band, for example, MODIS NIR band (841-876 nm) and SWIR band (2105 – 2155 nm). A previous study also evaluated MODIS NDVI and NDWI for vegetation drought monitoring, using Oklahoma Mesonet soil moisture data [14]. They carried out the correlation analysis between NDVI and FWI, NDWI and FWI over 4-month period (May 25 – September 30) in 2002-2006 at 17 Oklahoma Mesonet sites, and their results showed that FWI had slightly higher linear correlation with NDVI than NDWI, and they concluded that "NDVI is a more commonly used index and no additional benefit was gained by the NDWI" [14]. Note that plants usually respond to water stress in a gradual and adaptation process, and start to wilt at certain threshold value of soil moisture. In our study, we used the threshold approach and searched for appropriate threshold values from both soil moisture and water-related vegetation index. We used LSWI, calculated from MODIS NIR

band (841-876 nm) and SWIR band (1628 – 1652 nm). LSWI is highly correlated with NDWI, but LSWI does have unique feature, being positive for green vegetation and negative for senescent vegetation and soils. We used the shift (switch) of LSWI from positive values to negative values as an indicator of severe drought or water stress to vegetation, and it corresponds well with the drought definition from soil moisture (FWI $< 0.5$ in this study). The results from this study have demonstrated that the LSWI-based drought algorithm could predict reasonably well those areas affected by drought, with 3% commission error (false alarm) at the Oklahoma Mesonet sites during 2001-2010, when compared to the FWI-25 threshold, and 6% using FWI-60.

The comparison between MODIS-derived vegetation indices and soil moisture data from the Oklahoma Mesonet sites is complicated by spatial representations of these two measurement approaches [14]. The MODIS data we used in this study have a spatial resolution of 500-m, representing area-averaged measurements. The soil moisture data from the Oklahoma Mesonet sites are essentially point measurements. Spatial heterogeneity in vegetation and soils within MODIS pixels clearly affect the correlation analysis between vegetation indices and FWI [14], and the threshold analysis in this study. The omission error (as shown in Table 3 and Figure 8) in the LSWI- and FWI-based drought algorithm can be largely attributed to the issues related to the scale and spatial heterogeneity (soils, grass and trees) within MODIS pixels. In addition, soil texture and organic properties have high variability horizontally and vertically [47], [48], and this may also affect the relationship between soil moisture and LSWI in our analysis. The root zone of grassland vegetation varies substantially spatially ranging from peak root density in the top 10-30 cm [49], [50] to maximum rooting depths of 88-370 cm [49], [50], [51], [52] for temperate grasslands. Those sites with deeper root zones are likely to be more resistant to drought than those sites with shallow root zones, as vegetation can use additional water from deeper soils. Unfortunately, most Oklahoma Mesonet sites do not have data of soil depth and root zone, which limits the analysis between LSWI and FWI at 25-cm and 60-cm depth. It is possible that some grassland sites may have deeper root depth than 60-cm below the surface. For example, soil depth data at the Marena site could be as deep as 120 cm (Tyson Ochsner, personal communication; unpublished data). The heat dissipation sensors used to collect the soil moisture at the Mesonet sites do not perform very well on sandy soils [14], [36] and thus the relationship between FWI and LSWI may not be reliable at sites that are dominated by this soil type.

A new instrument, which uses cosmic-ray neutrons to measure soil moisture, has recently emerged, and represents a break-through to address the challenge of measuring soil moisture at the landscape scale [53], [54]. The cosmic-ray soil moisture probe is being developed [53], [54], namely the COsmic-ray Soil Moisture Observing System (COSMOS). The COSMOS instrument detects soil moisture within an area of ~36 ha (~660 m in diameter) at a depth of up to ~70 cm. Data collection rate is user defined and the instrument may sample at rates as fast as one minute. The COSMOS instrument has been deployed and evaluated at many sites across the United States as part of a growing COSMOS network (http://cosmos.hwr.arizona.edu).

Currently, a COSMOS station has been deployed near the Marena site as part of a multi-agency, multi-collaborator team studying the variability of soil moisture sensor technologies. As the COSMOS soil moisture measurement is comparable with MODIS-based vegetation indices, a comparison study between the COSMOS-based soil moisture and MODIS-derived vegetation indices in the near future will certainly shed new insight on the sensitivity and potential of the LSWI-based drought algorithm.

In summary, the results of this study show that LSWI is sensitive to summer drought in Oklahoma and LSWI-based drought algorithm performs reasonably well in identifying vegetation drought, with approximately 2% commission error (false alarm) for the homogenous grassland sites and 3% commission error for all the Oklahoma Mesonet sites using the FWI-25 drought threshold; and 6% and 9% respectively for the FWI-60 drought threshold. The LSWI-based drought algorithm provides detailed maps of vegetation drought, which could better serve stakeholders (e.g., farmers and ranchers), decision makers and the public for drought impact assessment.

Continuing evaluation of the LSWI-based drought algorithm and comparison with other vegetation drought monitoring tools [55], [56], [30], [14], [24], [13] will

help us to further improve it as a tool to map and track dynamics of vegetation drought.

## Acknowledgment

The authors thank all the members of the Earth Observation and Modeling Lab at the University of Oklahoma that helped during the course of this study.

## References

[1] Novick, K.A., Stoy, P.C., Katul, G.G., Ellsworth, D.S., Siqueira, M.B.S., Juang, J., & Oren, R. (2004). Carbon dioxide and water vapor exchange in a warm temperate grassland. Oecologia, 138, 259-274

[2] White, R.P., Murray, S., Rohweder, M. (2000). Pilot Analysis of Global Ecosystems: Grassland Ecosystems. In (p. 81): World Resources Institute White, R.P., Murray, S., Rohweder, M. (2000). Pilot Analysis of Global Ecosystems: Grassland Ecosystems. In (p. 81): World Resources Institute

[3] Conner, R., Seidl, A., VanTassell, L., Wilkins, N. (2001). United States Grasslands and Related Resources: An Economic and Biological Trends Assessment. In, US Grasslands: Economic & Biological Trends (p. 170). Austin: Texas A&M University

[4] Mayeux, H. (2001). The Extent, General Characteristics, and Carbon Dynamics of U.S. Grazing Lands. The potential of U.S. grazing lands to sequester carbon and mitigate greenhouse effect: Lewis Publishers, CRC Press LLC.

[5] Foody, G.M., & Dash, J. (2010). Estimating the relative abundance of C-3 and C-4 grasses in the Great Plains from multi-temporal MTCI data: issues of compositing period and spatial generalizability. International Journal of Remote Sensing, 31, 351-362

[6] Namias, J. (1982). Anatomy of Great Plains Protracted Heat Waves (especially the 1980 U.S. summer drought). Monthly Weather Review, 110, 824-838

[7] Trenberth, K.E., Branstator, G.W., & Arkin, P.A. (1988). Origins of the 1988 North American Drought. Science, 242, 1640-1645

[8] Hong, S.-Y., & Kalnay, E. (2000). Role of sea surface temperature and soil-moisture feedback in the 1998 Oklahoma-Texas drought. Nature, 408, 842-844

[9] Schubert, S.D., Suarez, M.J., Pegion, P.J., Koster, R.D., & Bacmeister, J.T. (2004). Causes of Long-Term Drought in the U.S. Great Plains. Journal of Climate, 17, 485-503

[10] Andreadis, K.M., Clark, E.A., Wood, A.W., Hamlet, A.F., & Lettenmaier, D.P. (2005). Twentieth-Century Drought in the Conterminous United States. Journal of Hydrometeorology, 6, 985-1001

[11] McCrary, R.R., & Randall, D.A. (2009). Great Plains Drought in Simulations of the Twentieth Century. Journal of Climate, 23, 2178-2196

[12] Wang, J. (2007). FPGA Design for Real-Time Implementation of Constrained Energy Minimization for Hyperspectral Target Detection. High Performance Computing in Remote Sensing: Chapman and Hall/CRC

[13] Zhang, X.Y., Goldberg, M., Tarpley, D., Friedl, M.A., Morisette, J., Kogan, F., & Yu, Y.Y. (2010). Drought-induced vegetation stress in southwestern North America. Environmental Research Letters, 5

[14] Gu, Y.X., Hunt, E., Wardlow, B., Basara, J.B., Brown, J.F., & Verdin, J.P. (2008). Evaluation of MODIS NDVI and NDWI for vegetation drought monitoring using Oklahoma Mesonet soil moisture data. Geophysical Research Letters, 35

[15] Palmer, W.C. (1965). Meteorological drought. In. Washington, D.C.: U.S. Department of Commerce Weather Bureau

[16] McKee, T.B., Doesken, N.J., & Kleist, J. (1993). The relationship of drought frequency and duration. In, Preprints, 8th Conference on Applied Climatology (pp. 179-184). Anaheim, CA

[17] McKee, T.B., Doesken, N.J., & Kleist, J. (1995). Drought monitoring with multiple time scales. In, Preprints, 9th Conference on Applied Climatology (pp. 233-236). Dallas, TX

[18] Anderson, L.O., Malhi, Y., Aragao, L., Ladle, R., Arai, E., Barbier, N., & Phillips, O. (2010). Remote

sensing detection of droughts in Amazonian forest canopies. New Phytologist, 187, 733-750

[19] Tucker, C.J., & Choudhury, B.J. (1987). SATELLITE REMOTE-SENSING OF DROUGHT CONDITIONS. Remote Sensing of Environment, 23, 243-251

[20] Bayarjargal, Y., Karnieli, A., Bayasgalan, M., Khudulmur, S., Gandush, C., & Tucker, C.J. (2006). A comparative study of NOAA-AVHRR derived drought indices using change vector analysis. Remote Sensing of Environment, 105, 9-22

[21] Gonzalez Alonso, F., Cuevas, J.M., Casanova, J.L., Calle, A., & Illera, P. (1995). Drought monitoring in Spain using satellite remote sensing. Sensors and environmental applications of remote sensing, 87-90

[22] Jain, S.K., Keshri, R., Goswami, A., & Sarkar, A. (2010). Application of meteorological and vegetation indices for evaluation of drought impact: a case study for Rajasthan, India. Natural Hazards, 54, 643-656

[23] Kamble, M.V., Ghosh, K., Rajeevan, M., & Samui, R.P. (2010). Drought monitoring over India through Normalized Difference Vegetation Index (NDVI). Mausam, 61, 537-546

[24] Kogan, F.N. (1997). Global drought watch from space. Bulletin of the American Meteorological Society, 78, 621-636

[25] Liu, W.T., & Juarez, R.I.N. (2001). ENSO drought onset prediction in northeast Brazil using NDVI. International Journal of Remote Sensing, 22, 3483-3501

[26] Murthy, C.S., Sai, M., Chandrasekar, K., & Roy, P.S. (2009). Spatial and temporal responses of different crop-growing environments to agricultural drought: a study in Haryana state, India using NOAA AVHRR data. International Journal of Remote Sensing, 30, 2897-2914

[27] Tucker, C.J. (1989). COMPARING SMMR AND AVHRR DATA FOR DROUGHT MONITORING. International Journal of Remote Sensing, 10, 1663-1672

[28] Karnieli, A., Agam, N., Pinker, R.T., Anderson, M., Imhoff, M.L., Gutman, G.G., Panov, N., & Goldberg, A. (2010). Use of NDVI and Land Surface Temperature for Drought Assessment: Merits and Limitations. Journal of Climate, 23, 618-633

[29] Gao, B.C. (1996). NDWI - A normalized difference water index for remote sensing of vegetation liquid water from space. Remote Sensing of Environment, 58, 257-266

[30] Gu, Y.X., Brown, J.F., Verdin, J.P., & Wardlow, B. (2007). A five-year analysis of MODIS NDVI and NDWI for grassland drought assessment over the central Great Plains of the United States. Geophysical Research Letters, 34, L06407

[31] Liu, C.L., Wu, B.F., Tian, Y.C., Xu, W.B., & Huang, J.X. (2004). Crop drought monitoring using serial NDVI&NDWI in Northern China. Igarss 2004: Ieee International Geoscience and Remote Sensing Symposium Proceedings, Vols 1-7, 2264-2267

[32] Xiao, X.M., Boles, S., Liu, J.Y., Zhuang, D.F., & Liu, M.L. (2002). Characterization of forest types in Northeastern China, using multi-temporal SPOT-4 VEGETATION sensor data. Remote Sensing of Environment, 82, 335-348

[33] Xiao, X.M., Hollinger, D., Aber, J., Goltz, M., Davidson, E.A., Zhang, Q.Y., & Moore, B. (2004). Satellite-based modeling of gross primary production in an evergreen needleleaf forest. Remote Sensing of Environment, 89, 519-534

[34] Kalfas, J.L., Xiao, X., Vanegas, D.X., Verma, S.B., & Suyker, A.E. (2011). Modeling gross primary production of irrigated and rain-fed maize using MODIS imagery and CO2 flux tower data. Agricultural and Forest Meteorology, 151, 1514-1528

[35] Illston, B.G., Basara, J.B., & Crawford, K.C. (2004). Seasonal to interannual variations of soil moisture measured in Oklahoma. International Journal of Climatology, 24, 1883-1896

[36] Illston, B.G., Basara, J.B., Fiebrich, C.A., Crawford, K.C., Hunt, E., Fisher, D.K., Elliott, R., & Humes, K. (2008). Mesoscale Monitoring of Soil Moisture across a Statewide Network. Journal of Atmospheric and Oceanic Technology, 25, 167-182

[37] McPherson, R.A., Fiebrich, C.A., Crawford, K.C., Elliott, R.L., Kilby, J.R., Grimsley, D.L., Martinez, J.E., Basara, J.B., Illston, B.G., Morris, D.A., Kloesel, K.A., Stadler, S.J., Melvin, A.D., Sutherland, A.J., Shrivastava, H., Carlson, J.D., Wolfinbarger, J.M., Bostic, J.P., & Demko, D.B. (2007). Statewide monitoring of the mesoscale environment: A technical update on the Oklahoma Mesonet. Journal of Atmospheric and Oceanic Technology, 24, 301-321

[38] Lillesand, T., Kiefer, R., Chipman, J. (2008). Remote sensing and image interpretation, 6th edition. (6 ed.). John Wiley & Sons New York

[39] Justice, C.O., Townshend, J.R.G., Vermote, E.F., Masuoka, E., Wolfe, R.E., Saleous, N., Roy, D.P., and Morisette, J.T. 2002. An overview of MODIS Land data processing and product status. Remote Sensing of Environment 83 (1-2):3-15

[40] Xiao, X.M., Boles, S., Frolking, S., Li, C.S., Babu, J.Y., Salas, W., & Moore, B. (2006). Mapping paddy rice agriculture in South and Southeast Asia using multi-temporal MODIS images. Remote Sensing of Environment, 100, 95-113

[41] Xiao, X.M., Boles, S., Liu, J.Y., Zhuang, D.F., Frolking, S., Li, C.S., Salas, W., & Moore, B. (2005). Mapping paddy rice agriculture in southern China using multi-temporal MODIS images. Remote Sensing of Environment, 95, 480-492

[42] Xiao, X.M., Zhang, Q.Y., Braswell, B., Urbanski, S., Boles, S., Wofsy, S., Berrien, M., & Ojima, D. (2004). Modeling gross primary production of temperate deciduous broadleaf forest using satellite images and climate data. Remote Sensing of Environment, 91, 256-270

[43] Schneider, J.M., Fisher, D.K., Elliott, R.L., Brown, G.O., & Bahrmann, C.P. (2003). Spatiotemporal variations in soil water: First results from the ARM SGP CART network. Journal of Hydrometeorology, 4, 106-120

[44] Dong, X., Xi, B., Kennedy, A., Feng, Z., Entin, J.K., Houser, P.R., Schiffer, R.A., L'Ecuyer, T., Olson, W.S., Hsu, K.-l., Liu, W.T., Lin, B., Deng, Y., & Jiang, T. (2011). Investigation of the 2006 drought and 2007 flood extremes at the Southern Great Plains through an integrative analysis of observations. Journal of Geophysical Research, 116

[45] Kogan, F.N. (1995). Droughts of the Late 1980s in the United-States as Derived from Noaa Polar-Orbiting Satellite Data. Bulletin of the American Meteorological Society, 76, 655-668

[46] Shakya, N., & Yamaguchi, Y. (2010). Vegetation, water and thermal stress index for study of drought in Nepal and central northeastern India. International Journal of Remote Sensing, 31, 903-912

[47] Basara, J.B., & Crawford, K.C. (2002). Linear relationships between root-zone soil moisture and atmospheric processes in the planetary boundary layer. Journal of Geophysical Research-Atmospheres, 107

[48] Famiglietti, J.S., Devereaux, J.A., Laymon, C.A., Tsegaye, T., Houser, P.R., Jackson, T.J., Graham, S.T., Rodell, M., & van Oevelen, P.J. (1999). Ground-based investigation of soil moisture variability within remote sensing footprints during the Southern Great Plains 1997 (SGP97) Hydrology Experiment. Water Resources Research, 35, 1839-1851

[49] Jackson, R.B., Canadell, J., Ehleringer, J.R., Mooney, H.A., Sala, O.E., & Schulze, E.D. (1996). A global analysis of root distributions for terrestrial biomes. Oecologia, 108, 389-411

[50] Sun, G., Coffin, D.P., & Lauenroth, W.K. (1997). Comparison of root distributions of species in North American grasslands using GIS. Journal of Vegetation Science, 8, 587-596

[51] Canadell, J., Jackson, R.B., Ehleringer, J.R., Mooney, H.A., Sala, O.E., & Schulze, E.D. (1996). Maximum rooting depth of vegetation types at the global scale. Oecologia, 108, 583-595

[52] Schulze, E.D., Mooney, H.A., Sala, O.E., Jobbagy, E., Buchmann, N., Bauer, G., Canadell, J., Jackson, R.B., Loreti, J., Oesterheld, M., & Ehleringer, J.R. (1996). Rooting depth, water availability, and vegetation cover along an aridity gradient in Patagonia. Oecologia, 108, 503-511

[53] Desilets, D., Zreda, M., & Ferre, T.P.A. (2010). Nature's neutron probe: Land surface hydrology at an elusive scale with cosmic rays. Water Resources Research, 46

[54] Zreda, M., Desilets, D., Ferre, T.P.A., & Scott, R.L. (2008). Measuring soil moisture content non-invasively at intermediate spatial scale using cosmic-ray neutrons. Geophysical Research Letters, 35

[55] Brown, J.F., Wardlow, B.D., Tadesse, T., Hayes, M.J., & Reed, B.C. (2008). The Vegetation Drought Response Index (VegDRI): A new integrated approach for monitoring drought stress in vegetation. Giscience & Remote Sensing, 45, 16-46

[56] Brown, M.E., Pinzon, J.E., Didan, K., Morisette, J.T., & Tucker, C.J. (2006). Evaluation of the consistency of long-term NDVI time series derived from AVHRR, SPOT-Vegetation, SeaWiFS, MODIS, and Landsat ETM+ sensors. Ieee Transactions on Geoscience and Remote Sensing, 44, 1787-1793

[57] Kogan, F.N. (2000). Satellite-observed sensitivity of world land ecosystems to El Nino/La Nina. Remote Sensing of Environment, 74, 445-462

## Los Autores

### Diana X. Vanegas

Environmental Engineer, El Bosque University (2006), Masters in Geoinformatics, University of Oklahoma – USA (2011). Work experience as the Environmental Engineer at a Local mayor office in Bogota DC (2006 - 2008); professional research assistant at Earth Observation and Modeling Facility (http://eomf.ou.edu/), the University of Oklahoma (2009-2012) and virtual teacher of the Environmental Engineering program at El Bosque University (2012-2014).

### Xiangming Xiao

Is a Professor of Ecology and Remote Sensing at the Department of Microbiology and Plant Biology (http://mpbio.ou.edu). His research interest include remote sensing, land use and land cover change, carbon cycle, and infectious disease ecology. He has published 150 papers and book chapters.

### Jeffrey Basara

Jeffrey Basara is an Associate Professor in the School of Meteorology (http://weather.ou.edu) at the University of Oklahoma and the Director of Research at the Oklahoma Climatological Survey. His research interests include the physical processes which impact land-atmosphere interactions, the planetary boundary layer, drought, flash floods, and urban meteorology.